Published in final edited form as:

*Cancer Res*. 2019 January 01; 79(1): 72–85. doi:10.1158/0008-5472.CAN-18-1304.

# Aberrant activation of β-catenin signaling drives glioma tumorigenesis via USP1-mediated stabilization of EZH2

**Li Ma**[1,2,†], **Kangyu Lin**[1,†], **Guoqiang Chang**[3], **Yiwen Chen**[4], **Chen Yue**[1], **Qing Guo**[1], **Sicong Zhang**[5], **Zhiliang Jia**[3], **Tony T. Huang**[6], **Aidong Zhou**[1,*], **Suyun Huang**[1,7,**]

[1]Department of Neurosurgery, The University of Texas MD Anderson Cancer Center, Houston, Texas, 77030, USA.

[2]Department of Neuro-oncology and Neurosurgery, National Clinical Research Center for Cancer, Tianjin Medical University Cancer Institute and Hospital, Tianjin, 300060, China.

[3]Department of Gastroenterology, Hepatology & Nutrition, The University of Texas MD Anderson Cancer Center, Houston, Texas, 77030, USA.

[4]Department of Bioinformatics and Computational Biology, The University of Texas MD Anderson Cancer Center, Houston, TX, 77030, USA.

[5]Department of Biochemistry and Molecular Biology, Rockefeller University, New York, NY, 10065, USA.

[6]Department of Biochemistry and Molecular Pharmacology, New York University School of Medicine, New York, NY, 10016, USA.

[7]Program in Cancer Biology, The University of Texas Graduate School of Biomedical Sciences at Houston, Houston, Texas, 77030, USA.

## Abstract

Aberrant activation of β-catenin signaling is a critical driver for tumorigenesis, but the mechanism underlying this activation is not completely understood. In this study, we demonstrate a critical role of β-catenin signaling in stabilization of Enhancer of Zeste Homolog 2 (EZH2) and control of EZH2-mediated gene repression in oncogenesis. β-catenin/TCF4 activated transcription of the deubiquitinase USP1, which then interacted with and deubiquitinated EZH2 directly. USP1-mediated stabilization of EZH2 promoted its recruitment to the promoters of CDKN1B, RUNX3, and HOXA5, resulting in enhanced enrichment of histone H3K27me3 and repression of target gene expression. In human glioma specimens, expression levels of nuclear β-catenin, USP1, and EZH2 correlated with one another. Depletion of β-catenin/USP1/EZH2 repressed glioma cell proliferation in vitro and tumor formation in vivo. Our findings indicate that a β-catenin-

*Corresponding author: A. Zhou, Department of Neurosurgery, The University of Texas MD Anderson Cancer Center, 1515 Holcombe Blvd., Houston, TX 77030. azhou@mdanderson.org. **Corresponding author: S. Huang, Department of Neurosurgery, The University of Texas MD Anderson Cancer Center, 1515 Holcombe Blvd., Houston, TX 77030. suhuang@mdanderson.org.
†These authors contributed equally to this work.

Competing financial interests

The authors declare no competing financial interests.

The authors declare no potential conflicts of interest.

USP1-EZH2 axis orchestrates the interplay between dysregulated β-catenin signaling and EZH2-mediated gene epigenetic silencing during glioma tumorigenesis.

**Keywords**

β-catenin; USP1; EZH2; Ubiquitination; Glioma Tumorigenesis

## Introduction

Hyperactivated β-catenin signaling is recognized as an event that occurs frequently in multiple cancer types (1). The canonical Wnt/β-catenin pathway is triggered by Wnt ligands, leading to co-activation of the Frizzled and LRP receptors, and consequent stabilization and translocation of β-catenin into the nucleus (2). Nuclear β-catenin binds to the transcription factor TCF/LEF and thereby activates gene expression (2,3). In glioblastoma (GBM), early evidences for the involvement of Wnt signaling came from the germline mutations of *APC* gene (4). Recently, frequent aberrant promoter hypermethylation of Wnt pathway inhibitor genes such as *SFRP1, SFRP2, DKK1* and *WIF1* have been reported in glioblastomas and *WNT3A* up-regulation has been demonstrated in 81.8% malignant astrocytic gliomas and in 33.3% glioblastoma cell lines (5). Our previous study has demonstrated that overexpression of FoxM1 in GBM controls β-catenin nuclear translocation and is required for tumor progression, and therefore reveals a novel mechanism for β-catenin activation (6). Moreover, dysregulated EGFR signaling, accounting for up to 60% GBM cases, drives β-catenin signaling activation (7,8). Thus, aberrant β-catenin activation is prevailing in GBM and is a critical driver for tumorigenesis.

Activated β-catenin signaling is linked to epigenetics to control gene expression (9). For instance, β-catenin interacts with histone H3 arginine 8 methyltransferase (Prmt2) to establish poised chromatin architecture and mark genes for later expression in the development of *Xenopus* (10). Moreover, β-catenin activation leads to an induction and stabilization of MLL, and the β-catenin-CBP-MLL complex is required to trigger H3K4 tri-methylation at promoters of self-renewal genes in tumor propagating cells (11). However, further study is required to better understand the roles of β-catenin signaling in chromatin remodeling and epigenetic gene regulation.

Enhancer of Zeste Homolog 2 (EZH2) is a catalytic subunit of the Polycomb group (PcG) complex that participates in transcriptional repression of specific genes by mediating the trimethylation of histone H3K27 (12). EZH2 is frequently overexpressed in glioblastoma (GBM) and correlated with aggressiveness and advanced tumor progression (13,14). The oncogenic roles of EZH2 are largely due to its ability to repress the expression of a cohort of downstream tumor suppressor genes through H3K27 trimethylation-mediated epigenetic silencing, including *HOXA5*, *RUNX3*, and *CDKN1B* (12,15,16). EZH2 is subjected to proteasome-ubiquitination degradation pathway, and multiple E3 ligases, including Smurf2, β-TrCP, CHIP, have been identified to mediate EZH2 degradation in different biological context (17–19). However, the regulation of EZH2 stability and its implication in PRC2-mediated methyl transferase activity in a cancer-specific context is not fully explored.

In this study, we have demonstrated a critical role of β-catenin signaling in the regulation of EZH2. We found that β-catenin induced the expression of USP1, which then interacted and deubiquitinated EZH2 directly to suppress the ubiquitin-proteasomal degradation of EZH2. Active β-catenin-induced stabilization of EZH2 repressed downstream tumor suppressor genes expression, and therefore promoted glioma cell proliferation and tumor progression. The β-catenin-USP1-EZH2 axis revealed in our study orchestrates hyperactivated β-catenin signaling and EZH2-mediated epigenetic gene silencing, which represents a critical mechanism during glioma tumorigenesis.

## Methods and Materials

### Plasmids and reagents

USP1, USP2, USP3, USP4, USP5, USP8, USP11, USP13, USP14, USP15, USP16, USP18, USP20, USP25, USP26, USP29, USP30, USP36, USP39, USP46, USP48 and USP50 expression plasmids were kindly provided by Dr. Jianhua Yang (Texas Children's Cancer Center). MYC-EZH2 was kindly provided by Dr. Haojie Huang (Mayo Clinic). MYC-USP1 wild type and mutant, WDR48 were from Dr. Tony T. Huang (New York University School of Medicine). USP1 and EZH2 cDNA were further cloned into pcDNA3-HA vector. The truncated mutants of EZH2 were constructed into pcDNA3-HA vector. MYC-EZH2-K421R was from Dr. Mien-Chie Hung (MD Anderson Cancer Center), and Y641F site mutagenesis was introduced using the QuikChange site-directed mutagenesis kit (Agilent Technologies). Lentiviral vector expressing stabilized EZH2 was achieved by cloning the CDS region of MYC-EZH2-K421R/Y641F into a pLVX-IRES-ZsGreen vector (Clontech). Long and short USP1 promoter plasmids were achieved by cloning the USP1 promoter region with corresponding primers into pGL3-basic vector (Promega). Mutant USP1 promoter plasmids were also introduced by the QuikChange site-directed mutagenesis kit (Agilent Technologies). Lentiviral shRNA plasmids targeting USP1 (#1: TRCN0000342330, #2:TRCN0000342331) and EZH2 (#1: TRCN0000293738, #2: TRCN0000286290) were purchased from Sigma. All plasmid constructions were confirmed by DNA sequencing analysis.

Cycloheximide (CHX), MG132 and β-catenin siRNAs were purchased from Sigma. Puromycin was purchased from EMD Biosciences. Recombinant human Wnt3α was purchased from R&D Systems. B-catenin inhibitor PRI-724 was from Selleckchem. Dual-Luciferase Reporter Assay System was from Promega. Antibodies used in this study are listed in Supplementary Table S1.

### Cell culture, transfection and treatment

SW1783, U87MG, LN18, HS683, LN229 and HEK293T cell lines were from American Type Culture Collection (ATCC). U251MG cell line was from Sigma. The immortalized NHA-E6/E7/hTERT cell line has been described previously (20). These cell lines were grown in Dulbecco's modified Eagle's medium supplemented with 10% bovine calf serum (HyClone). GSC11 cells were isolated from human glioblastoma specimens and cultured as previously described (21). β-catenin$^{+/+}$ and β-catenin$^{-/-}$ MEFs were provided by Dr. Xi He (Boston Children's Hospital) and cultured as previously described (21). Above cells were

passaged less than five times after receipt in our laboratory for relevant studies reported here. No cell lines used in this study were found in the database of commonly misidentified cell lines that is maintained by ICLAC and NCBI Biosample. Cell lines were authenticated by short tandem repeat profiling and were routinely tested for mycoplasma contamination in every six months. The latest test date was in May of 2018.

Transfections of plasmid and siRNAs were performed using Turbofect (R0531, Thermo Fisher Scientific) and X-tremeGENE siRNA transfection reagents (04476093001, Roche Diagnostics), respectively. For treatment, cells were plated in multi-well plates and treated with the indicated concentration of CHX, MG132, and Wnt3a for the indicated times.

For lentiviral production, pLKO.1 shRNA vector or pLVX vector, packing (psPAX2) and envelope (pMD2.G) plasmids were co-transfected into HEK293T cells using Turbofect transfect reagent. After 48 hour transfection, glioma cells were infected with viral particles. Stable clones were selected by culturing cells in medium with 2 μg/mL puromycin for 2 weeks.

### In vivo and in vitro deubiquitylation of EZH2

Transfected cells were treated with 20 μM MG132 for 6 hours. Cells were lysed using RIPA lysis buffer (50 mM Tris-base pH 6.8, 150 mM NaCl, 1% NP-40, 0.5% deoxycholic acid, 0.1% SDS, 10 mM NaF, 10mM dithiothreitol (DTT), 0.2 mM $Na_3VO_4$, 1% cocktail protease inhibitors, 1 mM phenylmethylsulfonyl fluoride (PMSF). Cell lysates were immunoprecipitated using the indicated antibodies and washed three times by RIPA buffer. To exclude nonspecific ubiquitin-modified species from the EZH2 complex, we washed the immunoprecipitates three times using a ubiquitylation wash buffer (50 mM Tris-base pH 6.8, 150 mM NaCl, 1% NP-40, 0.5% deoxycholic acid, 1M urea, 1mM N-ethylmaleimide (NEM), and protease inhibitors).

In vitro deubiquitylation of EZH2 by USP1 was performed as described previously. HEK293T cells were transfected with HA-EZH2 and Flag-ubiquitin and were treated with 20 μM MG132 for 6 hours. HA-EZH2 containing ubiquitylated HA-EZH2 was purified from the SDS-denatured extracts with HA-beads, the bound proteins were eluted with 1 mg/ml HA-peptides (Sigma) in RIPA buffer after extensive washing. The ubiquitylated EZH2 protein was incubated with recombinant USP1/WDR48 proteins (Ubiquigent Ltd) in deubiquitylation buffer (20 mM HEPES (pH 8.3), 20 mM NaCl, 100 mg/ml BSA, 500 mM EDTA, 1 mM DTT) at 37 ºC for 2 h.

### Nuclear protein extraction, Immunoprecipitation and western blotting

Nuclear proteins were extracted using the CelLytica NuCLEAR Extraction Kit (Sigma) according to the manufacturer's instructions. The extraction of total proteins was performed using immunoprecipitation lysis buffer (25 mM Tris-HCl pH 7.4, 150 mM NaCl, 1% NP-40 nonyl phenoxypolyethoxylethanol, 1 mM ethylenediaminetetraacetic acid, protease and phosphatase inhibitors), and immunoprecipitation or immunoblotting with corresponding antibodies was performed as described previously (21).

### Quantitative PCR

Total RNA was isolated using Trizol reagent (Invitrogen) from cells and cDNA was synthesized using the iScript™ Reverse Transcription Supermix (Bio-Rad). Two-step real-time PCR was performed using SYBR Select Master Mix (Life Technologies) and 7500 Real-Time PCR System (Life Technologies) according to the manufacturer's instructions. The primer sequences used for PCR are listed in Supplementary Information, Table S2. The expression of housekeeping gene, glyceraldehyde-3-phosphate dehydrogenase (GAPDH) in each sample was used as an internal control. All quantitative PCR results were from three independent assays.

### Chromatin immunoprecipitation (ChIP) assays

The ChIP assay was performed using the ChIP kit (Cell Signaling #9002). Cells were cross-linked with formaldehyde and subjected to ChIP assay according to the manufacturer's instructions. The ChIP DNA was subjected to quantitative PCR or electrophoresed on a 1.5% agarose gel. The primers used for PCR were listed in Supplementary Information, Table S2.

### Immunofluorescence and immunohistochemical analysis

For immunofluorescence, cells cultured on coverslips were fixed with 4% paraformldehyde in PBS for 10 min, followed by permeabilization with Triton X-100 for 15 min. Cells were then blocked by 10% goat serum in PBS for 2 h, and incubated with the indicated antibody overnight at 4 °C, followed by incubation with Alexa Fluor 488 goat anti-mouse IgG or Alexa Fluor 594 goat anti-rabbit IgG (Invitrogen) for 1 h at room temperature. Coverslips were mounted on slides using anti-fade mounting medium with DAPI. Immunofluorescence images were acquired on a deconvolutional microscope (Zeiss). For each channel, all images were acquired with the same settings.

For immunohistochemical staining, tissue slides (Biomax) were deparaffinized and rehydrated through an alcohol series. After microwave antigen retrieval, indicated antibody were incubated with the slides overnight at 4 °C. Staining was performed using the EnVision kit (DAKO). The quantification of the staining was evaluated according to the percentage of cells with positive nuclear staining and to the staining intensity as previously described (21).

### Measurement of promoter reporter activity

Glioma cells or MEFs were transfected with the indicated USP1 promoter reporters combined with siRNAs, Wnt3α or β-catenin-inhibitor. The USP1 promoter activity in these cells was normalized by co-transfecting a β-actin/Renilla luciferase reporter (pRL-TK) containing a full-length Renilla luciferase gene. The luciferase activity in the cells was quantified using a dual luciferase assay system (Promega) according to the manufacturer's instructions.

### Cell proliferation and cell viability assay

Cell proliferation assay was conducted using XTT (Sigma) or CCK8 (Dojindo) according to the manufacturer's instructions. SW1783 cells expressing indicated constructs ($2\times10^3$) and

GSC11 cells expressing indicated constructs (8–12 $\times 10^3$) were seeded into 96-well plate and cultured in corresponding medium for the indicated numbers of days. Then cells were incubated with XTT or CCK8 for 3 hours. The absorbance was measured at 450 nm using a microplate reader. Cell viability assay was conducted using CCK8 (Dojindo) according to the manufacturer's instructions.

### Cell cycle analysis

SW1783 or GSC11 cells expressing indicated constructs were harvested, washed with PBS, fixed with 75% ethanol overnight at 4 °C, and then incubated with RNase at 37 °C for 30 min. The cell nuclei were stained with propidium iodide for an additional 30 min and then analyzed by flow cytometry. The results are presented as the percentage of cells in each phase.

### Intracranial tumor assay

All mouse experiments were approved by the Institutional Animal Care and Use Committee of The University of Texas MD Anderson Cancer Center. GSC11 cells ($5\times10^5$), or SW1783 cells ($1\times10^6$) were injected intracranially into 6- to 8-week-old nude (nu/nu) mice (6 mice for each group) as previously described (21). The mice were euthanized 4 weeks (GSC11), or 6 weeks (SW1783) after glioma cells injection and the brains were removed, fixed in 4% formaldehyde, and embedded in paraffin. Tumor formation and phenotype was determined by histologic analysis of hematoxylin and eosin stained sections. Tumor volume was calculated using the formula $V= (\pi/6)\times a^2\times b$, where a and b are the shortest diameter and longest diameter, respectively. For glioma cells injected mice survival assay, another 8 mice for each group were injected intracranially. Animals were humanely killed when they were moribund; the remaining mice were killed 90 days (GSC11 implanted mice) or 120 days (SW1783 implanted mice) after glioma cells injection.

### Statistical analysis

Each experiment was repeated three times or more. If not mentioned, all data were presented as mean ± sem of three independent experiments, and the two-tailed Student's t-test was used to compare two groups for independent samples. A Pearson correlation test was performed to analyze the relationships between active β-catenin, USP1 and EZH2. Survival analysis was conducted using the Kaplan-Meier model with a two-sided log-rank test. The results for statistical significance tests were included in the legend of each figure. $P<0.05$ was considered as statistically significant.

## Results

### β-catenin stabilizes EZH2 protein by inhibiting its ubiquitination.

Our previous study has shown that the Wnt/β-catenin signaling pathway plays a critical role in sustaining glioma stem cells and glioma tumorigenesis (6). In an attempt to test the effect of β-catenin on EZH2 expression, we detected EZH2 protein levels in β-catenin wild-type (β-catenin$^{+/+}$) and β-catenin knockout (β-catenin$^{-/-}$) MEFs. We found that EZH2 was reduced in β-catenin$^{-/-}$ MEFs compared with β-catenin$^{+/+}$ MEFs, which led to decreased level of histone H3K27me3 in β-catenin$^{-/-}$ MEFs (Fig.1A). Accordingly, overexpression of

the constitutively active β-catenin-S33Y mutant upregulated EZH2 levels in both SW1783 and NHA cells (Fig.1B). This result was further confirmed in the patient-derived GSC11 cells using the β-catenin small interfering RNAs (siRNAs) (Fig.1C). However, β-catenin had no obvious effect on EZH2 mRNA levels (Fig.S1A–C), suggesting that β-catenin regulates EZH2 expression post-transcriptionally.

Some studies have shown that EZH2 is regulated by the ubiquitin-proteasome-dependent degradation pathway (17–19), which has been confirmed in our study (Fig.S1 D and E). To determine whether β-catenin regulates EZH2 protein stability, we measured the abundance of EZH2 in β-catenin$^{+/+}$ and β-catenin$^{-/-}$ MEFs treated with cycloheximide (CHX). We found EZH2 was greatly destabilized in the absence of β-catenin (Fig.1D). Accordingly, overexpression of the active β-catenin-S33Y promoted the stability of EZH2 protein (Fig.1E). We next investigated the effect of β-catenin on the ubiquitination of EZH2, and found that overexpression of β-catenin-S33Y reduced EZH2 ubiquitination in SW1783 cells (Fig.1F). These results together indicate that β-catenin stabilizes EZH2 protein by inhibiting its ubiquitination.

## USP1 stabilizes EZH2 protein in GBM cells.

As a reverse procedure of ubiquitination, protein deubiquitination critically regulates protein turnover. To identify the deuibiquitinases (DUBs) responsible for reversing EZH2 polyubiquitination, we screened a panel of 23 DUBs, which usually function as oncogenes or show high expression in central nervous system. We found that EZH2 protein level was upregulated by deubiquitinases USP1, USP11, USP16, and USP29 in HEK293T cells under CHX treatment (Fig.S2A). Because DUBs may regulate EZH2 expression indirectly through mechanisms other than the ubiquitin-proteasome pathway, we thus examined the effect of DUBs on EZH2 ubiquitination. Of those four DUBs, only USP1 significantly reduced the ubiquitination of EZH2 protein (Fig.S2B), indicating that USP1 may act as a deubiquitinase of EZH2.

We next assessed the effect of USP1 on EZH2 protein stability. Depletion of USP1 in U87MG and GSC11 cells decreased EZH2 protein level as determined by western blot analysis (Fig.2A). In addition, overexpression USP1 in HEK293T and SW1783 cells significantly upregulated EZH2 protein level as determined by immunofluorescent staining (Fig.2B). Accordingly, EZH2 was almost abolished in USP1-depleted cells as determined by immunofluorescent staining (Fig.S2C). However, USP1 had no effect on *EZH2* mRNA levels (Fig. S2 D and E). Moreover, depletion of USP1 promoted EZH2 degradation in both U87MG and GSC11 cells, whereas USP1 overexpression increased EZH2 stability (Fig.2 C and D). Consistently, the expression of EZH2 was positively correlated with USP1 expression in glioma cell lines, but not with WD-repeat protein WDR48, a binding partner of USP1 (22) (Fig.2E). These findings indicate that USP1 contributes to the stabilization of EZH2 in glioma cells.

## USP1 interacts with and deubiquitinates EZH2 directly.

We next detected the interaction between USP1 and EZH2. USP1 and EZH2 proteins co-localized in nucleus in glioma cells (Fig. S2C). In addition, USP1 co-immunoprecipitated

with EZH2 in HEK293T cells ectopically expressing both proteins (Fig.S3A). Moreover, reciprocal co-immunoprecipitation experiments showed that endogenous USP1 and EZH2 interacted with each other in U87MG and GSC11 cells (Fig.3A). To map the protein region in EZH2 that mediates its interaction with USP1, we constructed plasmids expressing a series of deletion mutants of EZH2 and found the protein residues 310–484 of EZH2 containing a SANT domain is required for its interaction with USP1 (Fig.3B).

We further evaluated the effect of USP1 on EZH2 ubiquitination. Overexpression of wild-type USP1 notably reduced the ubiquitination of EZH2 (lane 3, Fig.3C), and this effect was enhanced by further expressing WDR48, an USP1-binding partner enhancing the activity of USP1 (lane 4, Fig.3C). However, overexpression of WDR48 alone did not significantly reduce the endogenous ubiquitination of EZH2 (lane 7, Fig.3C). Moreover, overexpression of USP1-C90S, a catalytically inactive form of USP1 (23), did not alter EZH2 ubiquitination either in the presence of WDR48 or not (lane 5 and lane 6, Fig.3C). Accordingly, depletion of endogenous USP1 using two independent shRNAs promotes EZH2 ubiquitination in GSC11 and U87MG cells (Fig.3D and Fig.S3B). To address the question whether USP1 deubiquitinates EZH2 directly, ubiquitinated EZH2 was purified from HEK293T cells and incubated with USP1 and WDR48 proteins. We found that USP1/WDR48 decreased EZH2 ubiquitination, and the efficiency was increased with the amount of USP1/WDR48 proteins that were added to the reactions (Fig.3E). Thus, these results strongly support that USP1 interacts with and deubiquitinates EZH2 directly.

### β-catenin promotes EZH2 stability by activating USP1 transcription.

We sought to determine whether USP1 expression was regulated by β-catenin in GBM. First, we surveyed the *β-catenin, TCF4* and *USP1* mRNA expression levels in GBM utilizing the TCGA datasets. We found *USP1* mRNA levels were linearly correlated with *β-catenin* and *TCF4* mRNA levels in GBM, respectively (Fig.S4A). The linear correlation between *β-catenin* and *USP1* expression levels was observed in all GBM subtypes (Fig.S4B). Moreover, transfection of β-catenin-S33Y significantly increased USP1 mRNA level in SW1783 and NHA cells (Fig.4 A and B). This result was further confirmed by depleting β-catenin in U87MG cells (Fig.4C) and GSC11 cells (Fig.S4C). Accordingly, USP1 mRNA level was decreased in β-catenin$^{-/-}$ MEFs compared with β-catenin$^{+/+}$ MEFs (Fig.S4D). These results suggest that β-catenin activates USP1 transcription.

We next searched the promoter region of USP1 and found one potential LEF/TCF consensus binding sequence around 2000bp upstream the transcription start site of USP1. In addition, ChIP assay showed that β-catenin bound to USP1 promoter region and the binding capability was enhanced under Wnt3a treatment (Fig.4D). To further confirm the transcriptional regulation of USP1 by β-catenin on, we constructed two USP1 promoter reporters, Pro-L and Pro-S, of which Pro-S lack the upstream TCF4 binding element (Fig.4E). Reporter gene assays showed that Pro-L was actually more responsive to Wnt3a and β-catenin signal compared with Pro-S (Fig.4 F, G, H, and Fig.S4E). Moreover, we also constructed promoter reporter plasmids harboring mutations of the TCF4 binding site using the empirical algorithm (24). The result showed that β-catenin inhibitor PRI-724 could significantly inhibit the wide-type promoter activity whereas showed no impact on mutant

promoter reporters (Fig.4I). Also, the reporter gene activities of the wide-type promoter in β-catenin$^{-/-}$ MEFs was significantly lower than that in β-catenin$^{+/+}$ MEFs, whereas no great change of the reporter gene activities driving by the mutant promoter was observed between β-catenin$^{+/+}$ and β-catenin$^{-/-}$ MEFs (Fig.S4F).

We further assessed the effect of β-catenin on USP1 and EZH2 protein expression. As indicated in Fig.2E, the expression of β-catenin in different glioma cell lines showed good positive correlation with that of USP1 and EZH2. Both USP1 and EZH2 were upregulated under Wnt3a treatment in SW1783 and NHA cells (Fig.4J). Accordingly, depleting β-catenin in U87MG cell using shRNA could significantly downregulate the USP1 and EZH2 protein expression (Fig.4K). Further, EZH2 expression was decreased in β-catenin$^{-/-}$ compared with β-catenin$^{+/+}$ MEFs, and overexpression of USP1 in β-catenin$^{-/-}$ MEFs restored EZH2 level (Fig.S4G). Taken together, these results demonstrate that β-catenin transcriptionally activates USP1 expression to promote EZH2 protein level in glioma.

## USP1-mediated EZH2 stabilization represses downstream gene expression.

By catalyzing histone H3 lysine 27 tri-methylation (H3K27me3), EZH2 represses a series of tumor suppressor genes associated with tumorigenic properties of GBM, including *CDKN1B*, *RUNX3*, *HOXA5*. We therefore assessed the effect of USP1 on EZH2-mediated gene expression. Depletion of USP1 significantly decreased the recruitment of EZH2 on the promoters of *CDKN1B*, *RUNX3*, *HOXA5*, which led to decreased H3K27me3 levels on these promoters (Fig.5 A and B). We then measured the mRNA abundance of the EZH2 targets in the β-catenin/USP1/EZH2 context. In GSC11 cells, depletion of β-catenin/USP1/EZH2 increased the mRNA levels of those genes (Fig.5C). This result was further confirmed in SW1783 cells overexpressing Wnt3a (Fig.5D). Accordingly, the protein levels of p27 (a protein coded by *CDKN1B* gene), RUNX3, and HOXA5 were all upregulated by depletion of β-catenin/USP1/EZH2 in GSC11 cells (Fig.5E), and this result was further confirmed in SW1783 cells overexpressing Wnt3a (Fig.5F). Thus, these results together demonstrate that the β-catenin-USP1-EZH2 axis critically regulates target gene expression by controlling the H3K27me3 levels.

To further test the effect of USP1-EZH2 axis on the target protein expression, we constructed an EZH2 variant, EZH2–421R/641F, which is resistant to the proteasome-mediated protein degradation (17,18). We designate this variant as ND-EZH2 (Non-Degradation EZH2). Compared with the wide-type EZH2, ND-EZH2 was insensitive to CHX treatment (Fig.5G). Considering that the residue 421 of EZH2 is within the 310–484 region that mediates the interaction with USP1 (Fig.3B), it is probably that USP1 stabilizes EZH2 by reversing β-TrCP/Smurf2-mediated EZH2 ubiquitination. Moreover, overexpression of ND-EZH2 rescued the effect of USP1 depletion on the expression of RUNX3, HOXA5 and p27 (Fig.5H). These results support that USP1 promotes EZH2-mediated gene repression by stabilizing EZH2.

## The β-catenin/USP1/EZH2 axis promotes glioma tumorigenicity.

We further investigated the roles of the β-catenin-USP1-EZH2 axis in glioma cell proliferation and tumorigenesis. Depletion of USP1/EZH2 in SW1783 cells abolished

the effect of Wnt3a overproduction on cell proliferation, and reconstituted expression of the non-degradable EZH2 variant (ND-EZH2) reversed this effect (Fig.6A and Fig.S5A). Moreover, depletion of β-catenin/USP1/EZH2 in GSC11 cells markedly decreased cell proliferation, and reconstituted overexpression of ND-EZH2 almost fully reversed the effect of USP1 depletion (Fig.6B and Fig.S5B). Additionally, expression of the catalytically inactive EZH2 mutant (EZH2 ΔSET) rescued the effect of USP1 depletion on GSC11 proliferation, although to a less extent compared to restoring the full-length EZH2 (Fig.S5C). This result indicates that the non-catalytic function of EZH2 plays an important role in glioma cell proliferation, and the regulation of USP1 towards EZH2 is mediated by both EZH2's catalytic-dependent and -independent functions.

We next explored to determine whether the effect of β-catenin/USP1/EZH2 on cell proliferation was caused by the changes in cell cycle distribution. As we expected, Wnt3a overproduction in SW1783 cells significantly decreased the proportion of G0/G1 phase cells and increased G2/M phase cells (Fig.S5D). This effect was abolished by USP1 depletion, which was rescued by the reconstituted expression of ND-EZH2 (Fig.S5D). Accordingly, depletion of USP1/EZH2 in GSC11 cells markedly induced G0/G1 phase arrest, and reconstituted overexpression of ND-EZH2 reversed the effect of USP1 depletion on cell cycle distribution (Fig. S5E).

To investigate the functions of the β-catenin-USP1-EZH2 axis in tumor formation *in vivo*, we intracranially injected glioma cells into nude mice. SW1783 cells, which derived from lower grade glioma (grade III astrocytoma), didn't show tumor formation in nude mice (Fig.6C and Fig.S5F). However, overexpression of Wnt3a in the cells significantly promoted tumor growth, and the effect was largely reduced by USP1/EZH2 depletion (Fig.6C and Fig.S5F). Moreover, overexpression of ND-EZH2 further reversed the effects of USP1/EZH2 depletion on tumor formation (Fig. 6C). These results indicate that Wnt/β-catenin-USP1-EZH2 axis may play an important role in the malignant transition from glioma to GBM. Accordingly, all mice injected with GSC11 control cells developed tumors with characteristic GBM features. In contrast, depletion of β-catenin/USP1/EZH2 eliminated tumor formation, and the effect of USP1 depletion on tumor formation was rescued by the reconstituted expression of ND-EZH2 (Fig.6D and Fig.S5G). Furthermore, immunohistochemistry staining of mice brain tumor tissues confirmed that β-catenin/USP1-induced EZH2 stabilization was retained in these tumors (Fig.S5 H and I).

We next evaluated the effect of β-catenin/USP1/EZH2 axis on the survival of glioma-bearing mice. Overexpression of Wnt3a in SW1783 cells shortened the survival time of the implanted mice compared with the control, whereas depletion of USP1/EZH2 eliminated this effect (Fig.6E and Fig.S5J). Notably, reconstituted expression of ND-EZH2 further reversed the effect of USP1 depletion (Fig.6E). Moreover, depletion of β-catenin/USP1/EZH2 significantly extended the survival time of GSC11-GBM-bearing mice, whereas reconstituted expression of ND-EZH2 fully reversed the effect of USP1 depletion on mouse survival (Fig.6F and Fig.S5K).

Considering the remarkable roles of Wnt3a-EZH2 on glioma cell proliferation and tumorigenesis, we further investigated the genes that were involved in WNT3A-EZH2

pathway using IPA analysis (Ingenuity Pathway Analysis)[QIAGEN]. 330 experiment-validated genes downstream WNT3A (Fig.S6A and Excel S1 sheet 1), and 746 genes downstream EZH2 (Fig.S6B and Excel S1 sheet 2) were built and grown based on the Ingenuity Knowledge Database. 65 co-regulated genes downstream WNT3A and EZH2 were further screened out by “comparison” algorithm of the IPA software (Fig.S6C and Excel S1 sheet 3), and among them, 45 genes were associated with “cell proliferation of tumor cell lines” (Fig.S6D and Excel S1 sheet 4). Taken together, these results consistently demonstrate that the β-catenin-USP1-EZH2 axis plays a critical role in glioma cell proliferation and tumorigenesis.

### USP1 is upregulated in glioma patient samples and correlates with β-catenin activation and EZH2 level.

To determine the clinical relevance of our findings, we assessed the β-catenin/USP1/EZH2 protein expression in serial sections of 30 grade II-III astrocytoma and 50 GBM specimens. Expression level of USP1 was significantly correlated with nuclear β-catenin and EZH2 levels, respectively (Fig.7A and B, upper panel, $r=0.77$, $p<0.0001$; lower panel, $r=0.80$, $p<0.0001$). We next assessed whether the expression levels of nuclear β-catenin, USP1, and EZH2 correlated with the grade of glioma malignance in those specimens. We found that the expression levels of nuclear β-catenin, USP1 and EZH2 were significantly higher in GBM than in lower-grade astrocytoma (Fig.7C and D). Moreover, from the TCGA dataset, higher *USP1* mRNA expression levels predicted worse survival outcomes in glioma patients, and so did *EZH2* and *CTNNB1* (Fig.7E). These results suggest that β-catenin-USP1-EZH2 axis is functional in human gliomas.

## Discussion

As a classical view, activation of the β-catenin signaling enables β-catenin’s nuclear translocation to form a transactivation complex with the TCF/LEF1 family of transcription and activates downstream gene expression. In this study, we demonstrate a previously unrecognized role of β-catenin signaling, which stabilizes EZH2 and promotes the enrichment of H3K27me3 on target promoters, and thus mediates transcriptional gene silencing. Our study reveals a novel function for the dysregulated β-catenin signaling during tumorigenesis.

As a critical regulator of cell-cycle progression, stem cell maintenance, and tumorigenesis, the regulation of EZH2 expression and activity is intensively investigated. EZH2 mRNA expression is activated by the pRB-E2F pathway and c-Myc, but repressed by p53, leading to its overexpression in tumors (25–27). Moreover, EZH2 protein is phosphorylated by multiple protein kinases to regulate its H3K27 methyltransferase activity during cell cycle progression and oncogenesis (28, 29). Recently, EZH2 protein has been shown to be degraded through the ubiquitin-proteasome pathway by multiple E3 ubiquitin ligases under different biological context (17–19). As a reverse procedure of ubiquitination, protein deubiquitination is a tightly controlled process catalyzed by deubiquitinating enzymes and critically regulates protein turn-over (21, 30). During preparation of this manuscript, two other deubiquitinases, USP21 and ZRANB1, have been reported to stabilize EZH2

in different biology contexts. Chen Y. et al identify that USP21 can deubiquitinate and stabilize EZH2 to promote cell proliferation and metastasis in bladder carcinoma (31); Zhang P. et al find that ZRANB1 is an EZH2 deubiquitinase and regulates EZH2 function in breast cancer through both catalytic activity-dependent and -independent manner (32). Herein, our study identifies USP1 as a novel deubiquitinase which stabilizes EZH2 during glioma tumorigenesis, and demonstrates that the USP1-EZH2 axis plays a critical role in the malignant transformation of glioma cells.

A few studies have previously reported about the crosstalk between EZH2 and the Wnt/β-catenin signaling. On the one hand, EZH2 physically interacts with β-catenin and serves as a transcription co-activator to drive the expression of genes that are commonly targeted by Wnt signaling (33–35). On the other hand, EZH2 acts as the catalytic subunit of PRC2 that represses Wnt antagonist genes expression and thus causes hyper-activated β-catenin signaling (36). Our present study demonstrates that β-catenin signaling in turn induces EZH2 stabilization and promotes EZH2-mediated H3K27 trimethylation and gene silencing. Together, these findings thus indicate a β-catenin-EZH2 regulatory feedback loop, which may be a prevailing mechanism in oncogenesis.

The deubiquitinase USP1 plays a key role in cell cycle progression and genome integrity (37, 38). Some recent studies have reported the oncogenic functions of USP1 in multiple cancers. USP1 deubiquitylates inhibitors of DNA binding (ID) proteins and promotes stem cell-like characteristics in osteosarcoma (39), while USP1 inhibitor pomozide promotes ID1 degradation and inhibits leukemic cells growth (40). Moreover, USP1-deficient mice are resistant to Ras-driven skin tumors by elevating Fancd2 ubiquitination (41). During preparation of this manuscript, two additional studies have reported the roles of USP1 in glioblastoma stem cell maintenance and proneural glioma cell survival (42, 43). Our study here identifies the epigenetic modifier EZH2 as a new substrate of USP1. We find that overexpression of USP1 promotes EZH2-mediated repression of downstream tumor suppressor genes and GBM tumorigenesis, which thus expands our understanding of the functional mechanism of USP1 in tumorigenesis.

In summary, our study demonstrates a β-catenin-USP1-EZH2 axis orchestrating the hyperactivated β-catenin signaling and EZH2-mediated epigenetic gene silencing, which represents a critical mechanism for glioma tumorigenesis. Thus, targeting the axis may provide a new therapeutic strategy for glioblastoma.

## Supplementary Material

Refer to Web version on PubMed Central for supplementary material.

## Acknowledgements

We thank Dr. Jianhua Yang (Texas Children's Cancer Center) for providing DUB expressing plasmids, Dr. Mien-Chie Hung (MD Anderson Cancer Center) for providing MYC-EZH2-K421R plasmid, and Dr. Xi He (Boston Children's Hospital) for providing β-catenin$^{+/+}$ and β-catenin$^{-/-}$ MEFs. This work was supported in part by US NIH grants R01CA182684, R01CA201327, R01CA220236, and P50 CA127001-06.

## Reference


1. Nusse R, Clevers H. Wnt/beta-Catenin Signaling, Disease, and Emerging Therapeutic Modalities. Cell 2017;169:985–99 [PubMed: 28575679]
2. MacDonald BT, Tamai K, He X. Wnt/beta-catenin signaling: components, mechanisms, and diseases. Developmental cell 2009;17:9–26 [PubMed: 19619488]
3. Hurlstone A, Clevers H. T-cell factors: turn-ons and turn-offs. The EMBO journal 2002;21:2303–11 [PubMed: 12006483]
4. Mori T, Nagase H, Horii A, Miyoshi Y, Shimano T, Nakatsuru S, et al. Germ-line and somatic mutations of the APC gene in patients with Turcot syndrome and analysis of APC mutations in brain tumors. Genes, chromosomes & cancer 1994;9:168–72 [PubMed: 7515658]
5. Denysenko T, Annovazzi L, Cassoni P, Melcarne A, Mellai M, Schiffer D. WNT/beta-catenin Signaling Pathway and Downstream Modulators in Low- and High-grade Glioma. Cancer genomics & proteomics 2016;13:31–45 [PubMed: 26708597]
6. Zhang N, Wei P, Gong A, Chiu WT, Lee HT, Colman H, et al. FoxM1 promotes beta-catenin nuclear localization and controls Wnt target-gene expression and glioma tumorigenesis. Cancer cell 2011;20:427–42 [PubMed: 22014570]
7. Hu T, Li C. Convergence between Wnt-beta-catenin and EGFR signaling in cancer. Molecular cancer 2010;9:236 [PubMed: 20828404]
8. Cloughesy TF, Cavenee WK, Mischel PS. Glioblastoma: from molecular pathology to targeted treatment. Annual review of pathology 2014;9:1–25
9. Mosimann C, Hausmann G, Basler K. Beta-catenin hits chromatin: regulation of Wnt target gene activation. Nature reviews Molecular cell biology 2009;10:276–86 [PubMed: 19305417]
10. Blythe SA, Cha SW, Tadjuidje E, Heasman J, Klein PS. beta-Catenin primes organizer gene expression by recruiting a histone H3 arginine 8 methyltransferase, Prmt2. Developmental cell 2010;19:220–31 [PubMed: 20708585]
11. Wend P, Fang L, Zhu Q, Schipper JH, Loddenkemper C, Kosel F, et al. Wnt/beta-catenin signalling induces MLL to create epigenetic changes in salivary gland tumours. The EMBO journal 2013;32:1977–89 [PubMed: 23736260]
12. Cao R, Wang L, Wang H, Xia L, Erdjument-Bromage H, Tempst P, et al. Role of histone H3 lysine 27 methylation in Polycomb-group silencing. Science 2002;298:1039–43 [PubMed: 12351676]
13. Suva ML, Riggi N, Janiszewska M, Radovanovic I, Provero P, Stehle JC, et al. EZH2 is essential for glioblastoma cancer stem cell maintenance. Cancer research 2009;69:9211–8 [PubMed: 19934320]
14. Lee J, Son MJ, Woolard K, Donin NM, Li A, Cheng CH, et al. Epigenetic-mediated dysfunction of the bone morphogenetic protein pathway inhibits differentiation of glioblastoma-initiating cells. Cancer cell 2008;13:69–80 [PubMed: 18167341]
15. Fujii S, Ito K, Ito Y, Ochiai A. Enhancer of zeste homologue 2 (EZH2) down-regulates RUNX3 by increasing histone H3 methylation. The Journal of biological chemistry 2008;283:17324–32 [PubMed: 18430739]
16. Melnick A. Epigenetic therapy leaps ahead with specific targeting of EZH2. Cancer cell 2012;22:569–70 [PubMed: 23153531]
17. Sahasrabuddhe AA, Chen X, Chung F, Velusamy T, Lim MS, Elenitoba-Johnson KS. Oncogenic Y641 mutations in EZH2 prevent Jak2/beta-TrCP-mediated degradation. Oncogene 2015;34:445–54 [PubMed: 24469040]
18. Yu YL, Chou RH, Shyu WC, Hsieh SC, Wu CS, Chiang SY, et al. Smurf2-mediated degradation of EZH2 enhances neuron differentiation and improves functional recovery after ischaemic stroke. EMBO molecular medicine 2013;5:531–47 [PubMed: 23526793]
19. Wang X, Cao W, Zhang J, Yan M, Xu Q, Wu X, et al. A covalently bound inhibitor triggers EZH2 degradation through CHIP-mediated ubiquitination. The EMBO journal 2017;36:1243–60 [PubMed: 28320739]
20. Sonoda Y, Ozawa T, Hirose Y, Aldape KD, McMahon M, Berger MS, et al. Formation of intracranial tumors by genetically modified human astrocytes defines four pathways critical in

the development of human anaplastic astrocytoma. Cancer research 2001;61:4956–60 [PubMed: 11431323]

21. Zhou A, Lin K, Zhang S, Chen Y, Zhang N, Xue J, et al. Nuclear GSK3beta promotes tumorigenesis by phosphorylating KDM1A and inducing its deubiquitylation by USP22. Nature cell biology 2016;18:954–66 [PubMed: 27501329]
22. Goncalves JM, Cordeiro MMR, Rivero ERC. The Role of the Complex USP1/WDR48 in Differentiation and Proliferation Processes in Cancer Stem Cells. Current stem cell research & therapy 2017;12:416–22 [PubMed: 28302046]
23. Jung JK, Jang SW, Kim JM. A novel role for the deubiquitinase USP1 in the control of centrosome duplication. Cell Cycle 2016;15:584–92 [PubMed: 26822809]
24. Smith TF, Waterman MS. Identification of common molecular subsequences. Journal of molecular biology 1981;147:195–7 [PubMed: 7265238]
25. Bracken AP, Pasini D, Capra M, Prosperini E, Colli E, Helin K. EZH2 is downstream of the pRB-E2F pathway, essential for proliferation and amplified in cancer. The EMBO journal 2003;22:5323–35 [PubMed: 14532106]
26. Tang X, Milyavsky M, Shats I, Erez N, Goldfinger N, Rotter V. Activated p53 suppresses the histone methyltransferase EZH2 gene. Oncogene 2004;23:5759–69 [PubMed: 15208672]
27. Koh CM, Iwata T, Zheng Q, Bethel C, Yegnasubramanian S, De Marzo AM. Myc enforces overexpression of EZH2 in early prostatic neoplasia via transcriptional and post-transcriptional mechanisms. Oncotarget 2011;2:669–83 [PubMed: 21941025]
28. Cha TL, Zhou BP, Xia W, Wu Y, Yang CC, Chen CT, et al. Akt-mediated phosphorylation of EZH2 suppresses methylation of lysine 27 in histone H3. Science 2005;310:306–10 [PubMed: 16224021]
29. Wei Y, Chen YH, Li LY, Lang J, Yeh SP, Shi B, et al. CDK1-dependent phosphorylation of EZH2 suppresses methylation of H3K27 and promotes osteogenic differentiation of human mesenchymal stem cells. Nature cell biology 2011;13:87–94 [PubMed: 21131960]
30. Zhou A, Lin K, Zhang S, Ma L, Xue J, Morris SA, et al. Gli1-induced deubiquitinase USP48 aids glioblastoma tumorigenesis by stabilizing Gli1. EMBO reports 2017;18:1318–30 [PubMed: 28623188]
31. Chen Y, Zhou B, Chen D. USP21 promotes cell proliferation and metastasis through suppressing EZH2 ubiquitination in bladder carcinoma. Onco Targets and therapy 2017;10:681–689
32. Zhang P, Xiao Z, Wang S, Zhang M, Wei Y, Hang Q, et al. ZRANB1 Is an EZH2 Deubiquitinase and a Potential Therapeutic Target in Breast Cancer. Cell reports 2018;23:823–837 [PubMed: 29669287]
33. Shi B, Liang J, Yang X, Wang Y, Zhao Y, Wu H, et al. Integration of estrogen and Wnt signaling circuits by the polycomb group protein EZH2 in breast cancer cells. Molecular and cellular biology 2007;27:5105–19 [PubMed: 17502350]
34. Li X, Gonzalez ME, Toy K, Filzen T, Merajver SD, Kleer CG. Targeted overexpression of EZH2 in the mammary gland disrupts ductal morphogenesis and causes epithelial hyperplasia. The American journal of pathology 2009;175:1246–54 [PubMed: 19661437]
35. Jung HY, Jun S, Lee M, Kim HC, Wang X, Ji H, et al. PAF and EZH2 induce Wnt/beta-catenin signaling hyperactivation. Molecular cell 2013;52:193–205 [PubMed: 24055345]
36. Cheng AS, Lau SS, Chen Y, Kondo Y, Li MS, Feng H, et al. EZH2-mediated concordant repression of Wnt antagonists promotes beta-catenin-dependent hepatocarcinogenesis. Cancer research 2011;71:4028–39 [PubMed: 21512140]
37. Ogrunc M, Martinez-Zamudio RI, Sadoun PB, Dore G, Schwerer H, Pasero P, et al. USP1 Regulates Cellular Senescence by Controlling Genomic Integrity. Cell reports 2016;15:1401–11 [PubMed: 27160904]
38. Nijman SM, Huang TT, Dirac AM, Brummelkamp TR, Kerkhoven RM, D'Andrea AD, et al. The deubiquitinating enzyme USP1 regulates the Fanconi anemia pathway. Molecular cell 2005;17:331–9 [PubMed: 15694335]
39. Williams SA, Maecker HL, French DM, Liu J, Gregg A, Silverstein LB, et al. USP1 deubiquitinates ID proteins to preserve a mesenchymal stem cell program in osteosarcoma. Cell 2011;146:918–30 [PubMed: 21925315]

40. Mistry H, Hsieh G, Buhrlage SJ, Huang M, Park E, Cuny GD, et al. Small-molecule inhibitors of USP1 target ID1 degradation in leukemic cells. Molecular cancer therapeutics 2013;12:2651–62 [PubMed: 24130053]

41. Park E, Kim H, Kim JM, Primack B, Vidal-Cardenas S, Xu Y, et al. FANCD2 activates transcription of TAp63 and suppresses tumorigenesis. Molecular cell 2013;50:908–18 [PubMed: 23806336]

42. Lee JK, Chang N, Yoon Y, Yang H, Cho H, Kim E, et al. USP1 targeting impedes GBM growth by inhibiting stem cell maintenance and radioresistance. Neuro-oncology 2016;18:37–47 [PubMed: 26032834]

43. Rahme GJ, Zhang Z, Young AL, Cheng C, Bivona EJ, Fiering SN, et al. PDGF Engages an E2F-USP1 Signaling Pathway to Support ID2-Mediated Survival of Proneural Glioma Cells. Cancer research 2016;76:2964–76 [PubMed: 26951930]

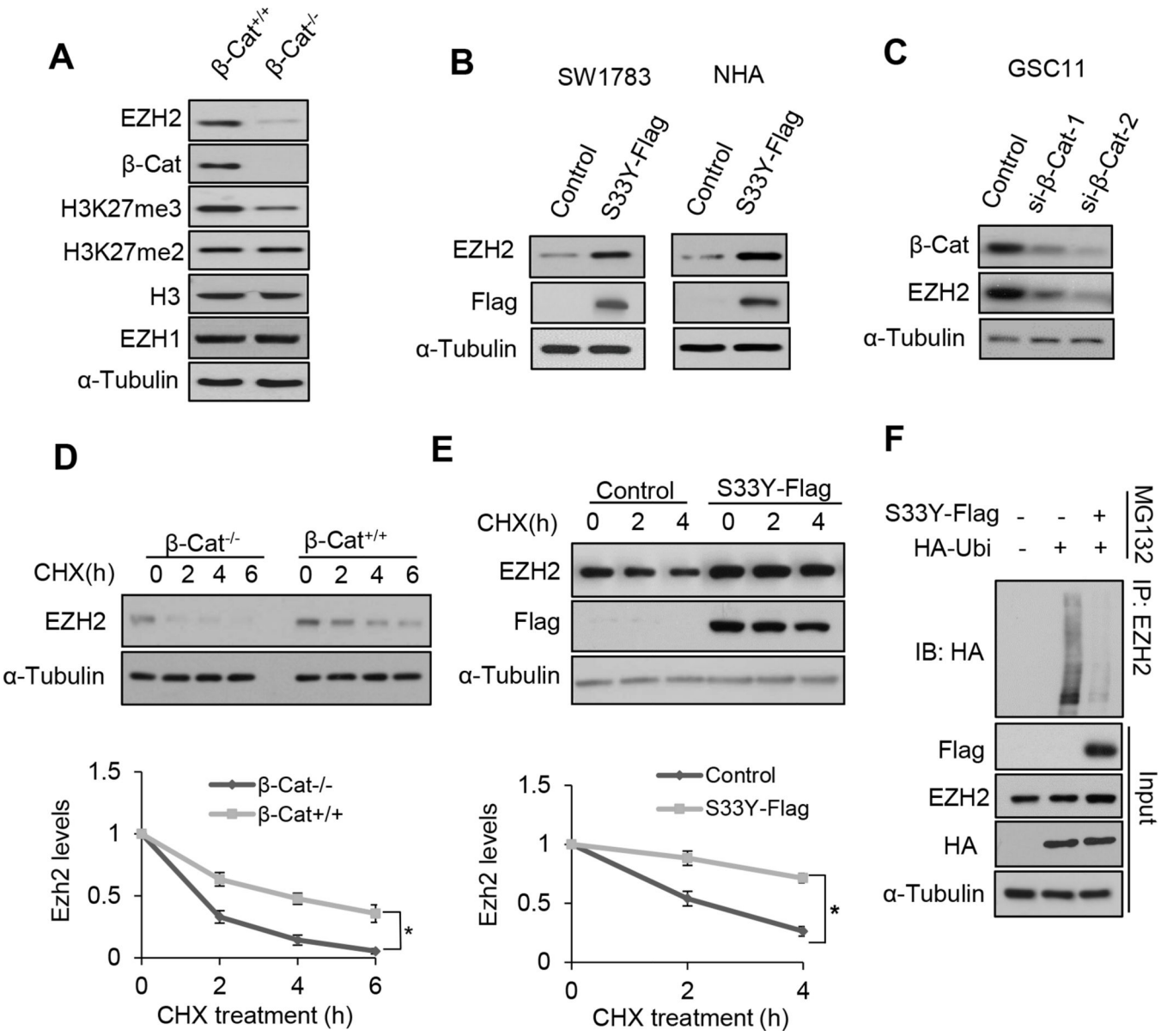


**Fig. 1. β-catenin stabilizes EZH2 by inhibiting its ubiquitination.**

**(A)** Immunoblotting of EZH2, β-catenin, H3K27me3 and H3K27me2 in β-Cat$^{-/-}$ and β-Cat$^{+/+}$ MEFs. EZH1, histone H3 and α-tubulin were used as loading controls. **(B)** NHA or SW1783 cells were transfected with β-catenin-S33Y-Flag plasmid and EZH2 expression was examined by immunoblotting. **(C)** GSC11 cells were transfected with two independent siRNAs against β-catenin and EZH2 was detected by immunoblotting. **(D)** MEFs were treated with 50 ng/ml CHX for the indicated time intervals and EZH2 expression was detected by immunoblotting. **(E)** SW1783 cells were transfected with β-catenin-S33Y-flag plasmid and then treated with 50 ng/ml CHX for the indicated time intervals. EZH2 expression was detected by immunoblotting. In (D) and (E), western blot band intensity of EZH2 was quantified and normalized to the internal control (mean ± s.d., n=3 independent experiments, Student's t-test). **(F)** SW1783 cells were transfected with β-catenin-S33Y-flag

and HA-Ubi, and then treated with MG132 (20 μM) for 6 h before harvest. Cell lysates were immunoprecipitated with an anti-EZH2 antibody and EZH2 ubiquitination was analyzed by immunoblotting.

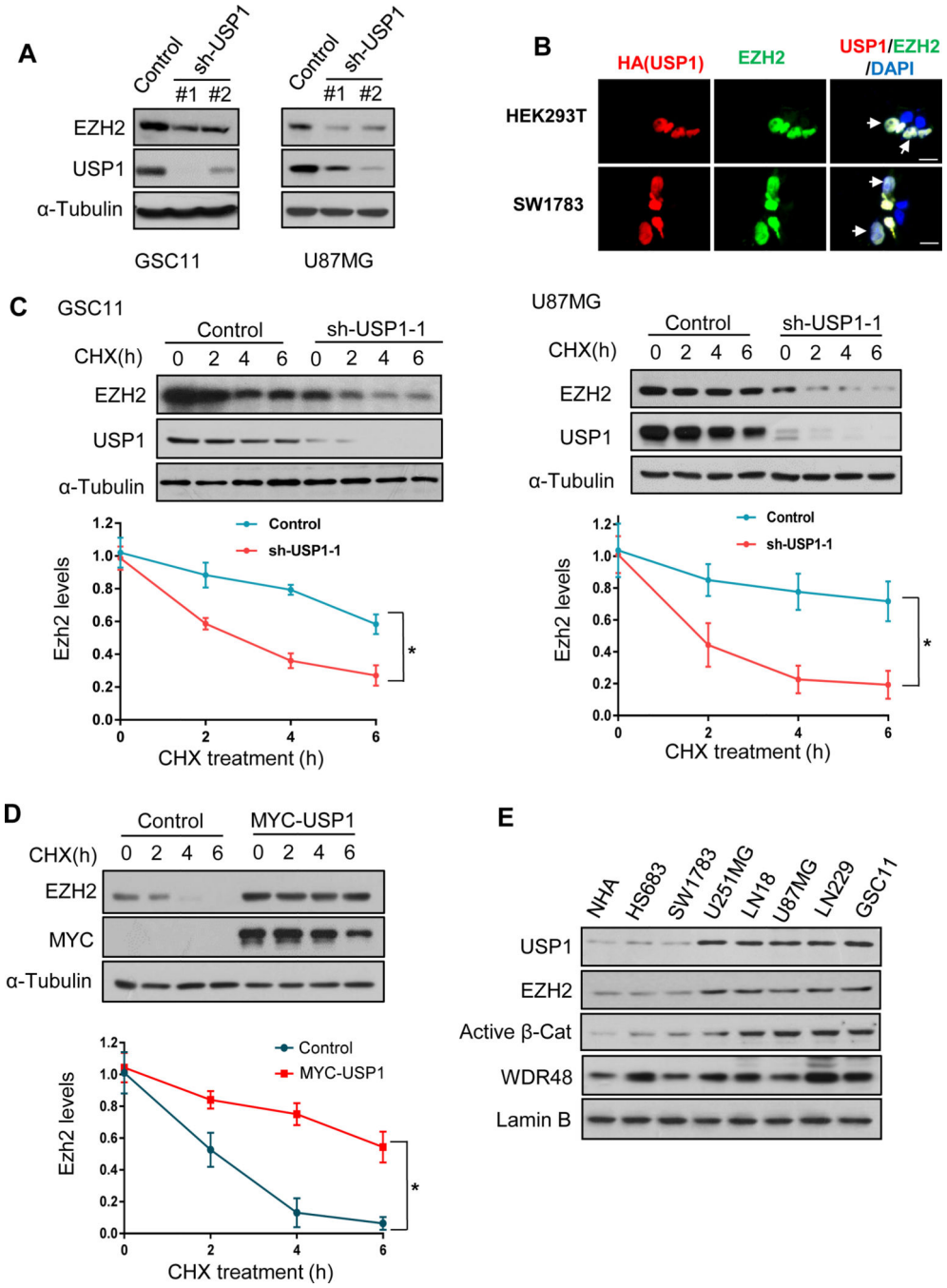


**Fig. 2. USP1 stabilizes EZH2 in GBM cells.**

**(A)** U87MG and GSC11 cells expressing two independent shRNAs of USP1 were analyzed by immunoblotting using the indicated antibodies. **(B)** HEK293T (upper) or SW1783 (lower) cells expressing HA-USP1 were co-cultured with the corresponding control cells, and representative images of immunofluorescent staining of EZH2 (green) and HA (red) were shown. Arrows indicate HA-USP1 transfected cells. **(C) - (D)** GSC11 cells expressing USP1 shRNA (C, left), U87MG cells expressing USP1 shRNA (C, right) and SW1783 cells expressing MYC-USP1(D) were treated with 50 ng/ml CHX for the indicated time intervals.

Cell lysates were analyzed by immunoblotting. Western blot band intensity of EZH2 was quantified and normalized to the internal control (mean ± s.d., n=3 independent experiments, Student's t-test, *P<0.05). **(E)** Immunoblotting analysis of protein levels of USP1, EZH2, active β-catenin and WDR48 in Normal Human Astrocytes (NHA), cell lines from lower grade gliomas and GBMs. Lamin B was used as nuclear fragment control.

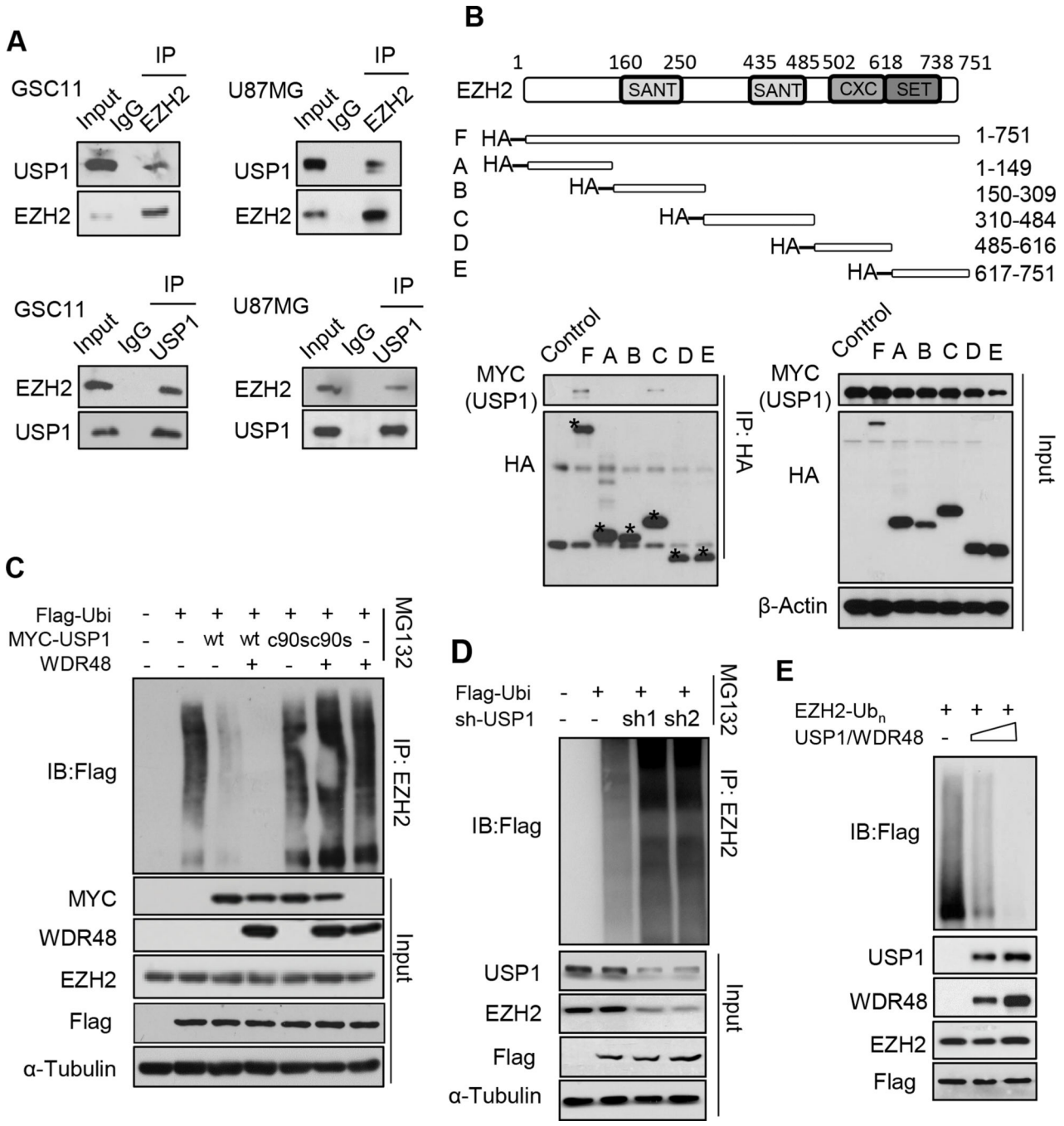


**Fig. 3. USP1 interacts with and deubiquitinates EZH2 directly.**

**(A)** GSC11 and U87MG cell lysates were immunoprecipitated with an anti-EZH2 or USP1 antibody, and the immunoprecipitates were analyzed by immunoblotting using the indicated antibodies. **(B)** A series of EZH2 deletion constructs were generated and co-transfected with MYC-USP1 into HEK293T cells. The cell lysates were immunoprecipitated with an anti-HA antibody and then subjected to immunoblotting analysis. Stars indicated principal, not non-specific western bands in this IP result. **(C)** HEK293T cells were transfected with MYC-USP1-wt or MYC-USP1-c90s, WDR48, and Flag-Ubi expressing plasmids, and

followed by treatment with MG132 (20 μM) for 6 h before cell harvest. Cell lysates were immunoprecipitated with EZH2 antibody and then analyzed by immunoblotting using the indicated antibodies. **(D)** GSC11 cells were transfected with USP1-shRNA and Flag-Ubi expressing plasmids, followed by treatment with MG132 (20 μM) for 6 h before cell harvest. Cell lysates were immunoprecipitated with EZH2 antibody and then analyzed by immunoblotting using the indicated antibodies. **(E)** HEK293T cells were transfected with HA-EZH2 and Flag-Ubi and then treated with MG132 (20 μM) for 6 h. EZH2 protein was purified using a HA-tag antibody. The ubiquitinated-EZH2 (EZH2-$Ub_n$) was then incubated with 50 ng or 500 ng USP1/WDR48 in a deubiquitination buffer. The resulting reactions were subjected to immunoblotting analysis.

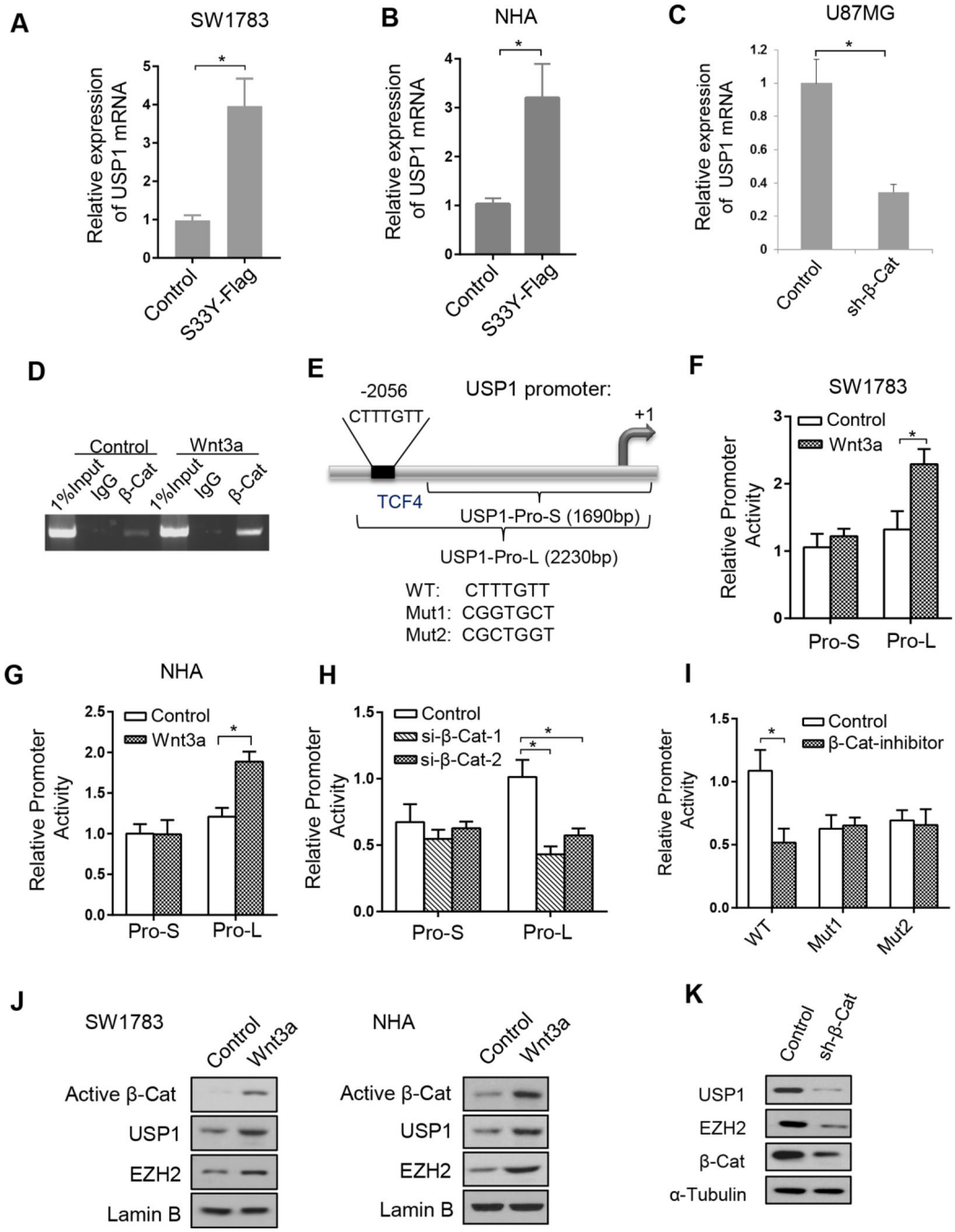


**Fig. 4. β-catenin promotes EZH2 stability by activating USP1 transcription.**

**(A)** and **(B)** SW1783 cells (A) and NHA cells (B) were transfected with Flag-β-catenin-S33Y and USP1 mRNA was detected by qRT-PCR. Data were mean ± s.d. of n=3 independent experiments, *P<0.05, Student's t-test. **(C)** USP1 mRNA in U87MG cells expressing β-catenin shRNA were detected by qPCR. Values were mean ± s.e.m. of n=3 independent experiments, *P<0.05, Student's t-test. **(D)** SW1783 cells were treated with or without Wnt3a (100ng/ml) for 24 hours. Cell lysates were subjected to chromatin immunoprecipitation analysis using anti-β-catenin antibody and the resultant DNAs was

analyzed by semi-quantitative PCR. **(E)** Scheme shows the USP1 promoter. Two promoter regions with different length (Pro-L and Pro-S) upstream the transcriptional start site (TSS) were cloned into the reporter plasmid. The sequences of wild-type and mutant TCF4 binding sites were indicated. **(F)** and **(G)** SW1783 cells (F) and NHA (G) were transfected with Pro-L or Pro-S plasmid, and then treated with Wnt3a (100 ng/ml) for 24 h. **(H)** U87MG cells were transfected with two independent siRNAs against β-catenin together with the Pro-L or Pro-S plasmid. From (F) to (H), reporter gene activities were measured by dual luciferase assays. Renilla luciferase (pRL-TK) was used as an internal control. Data were mean ± s.e.m., n=3 independent experiments, Student's t-test. *P<0.05. **(I)** U87MG cells were transfected with USP1 promoter reporter plasmids harboring wild-type (WT) or mutant TCF4 binding site(Mut), and then treated with a β-catenin inhibitor (PRI-724, 500nM) for 24 h. The relative promoter activities were evaluated by dual-luciferase assays. Values were mean ± s.e.m. of n=3 independent experiments, *P<0.05. **(J)** SW1783 cells or NHA cells were treated with 100 ng/ml Wnt3a for 48 hours, and the nuclear fragment were evaluated by immunoblotting using the indicated antibodies. Lamin B was used as nuclear fragment control. **(K)** U87MG cells expressing β-catenin shRNA were analyzed by immunoblotting using the indicated antibodies.

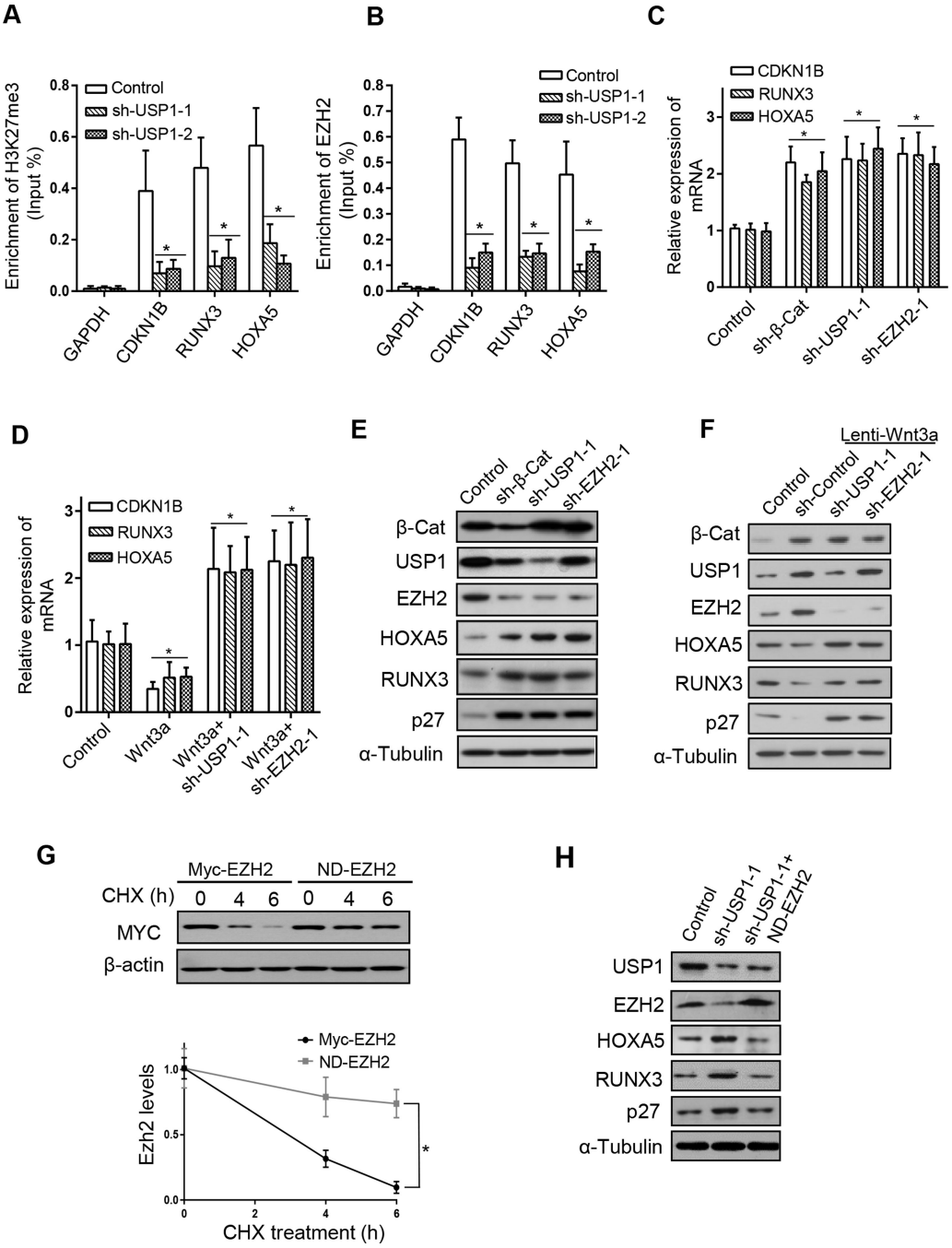


**Fig. 5. USP1-mediated EZH2 stabilization represses downstream gene expression.**

**(A)** and **(B)** GSC11 cells expressing USP1 shRNAs were analyzed by ChIP assays using an anti-H3K27me3 antibody (A) or anti-EZH2 antibody (B). The immunoprecipitated DNA was subjected to real-time qPCR analysis using primers in the promoter regions of *CDKN1B*, *RUNX3* and *HOXA5*. GAPDH locus was used as a negative control. Values are the percentage to input (mean ± s.e.m., n=3 independent experiments, Student's t-test. *P<0.05). **(C)** mRNA levels of *CDKN1B*, *RUNX3*, and *HOXA5* were analyzed by real-time PCR in GSC11 cells expressing the indicated shRNAs. **(D)** mRNA levels of *CDKN1B*,

*RUNX3*, and *HOXA5* in Control, Wnt3a, Wnt3a+shUSP1 and Wnt3a+shEZH2 transduced SW1783 cells were analyzed by real-time PCR. In (C) and (D), GAPDH was used as an internal control. Data were mean ± s.e.m. of n=3 independent experiments, Student's t-test. *P<0.05. **(E)** GSC11 cells stably expressing the indicated shRNAs were analyzed by immunoblotting using the indicated antibodies. **(F)** SW1783 cells expressing wnt3a were further overexpressed USP1 or EZH2 shRNA, and cell lysates were analyzed by immunoblotting using the indicated antibodies. **(G)** GSC11 cells were transfected with wide-type EZH2 (Myc-EZH2) or mutant EZH2 (Myc-EZH2–421R/641F) and then treated with 50 ng/ml CHX for the indicated time interval. The cell lysates were analyzed by immunoblotting using the indicated antibodies. Western blot band intensity of EZH2 was quantified and normalized to the internal control (mean ± s.d., n=3 independent experiments, Student's t-test, *P<0.05). **(H)** GSC11 cells expressing USP1 shRNA were reconstituted by the expression of ND-EZH2, and cell lysates were analyzed by immunoblotting using the indicated antibodies.

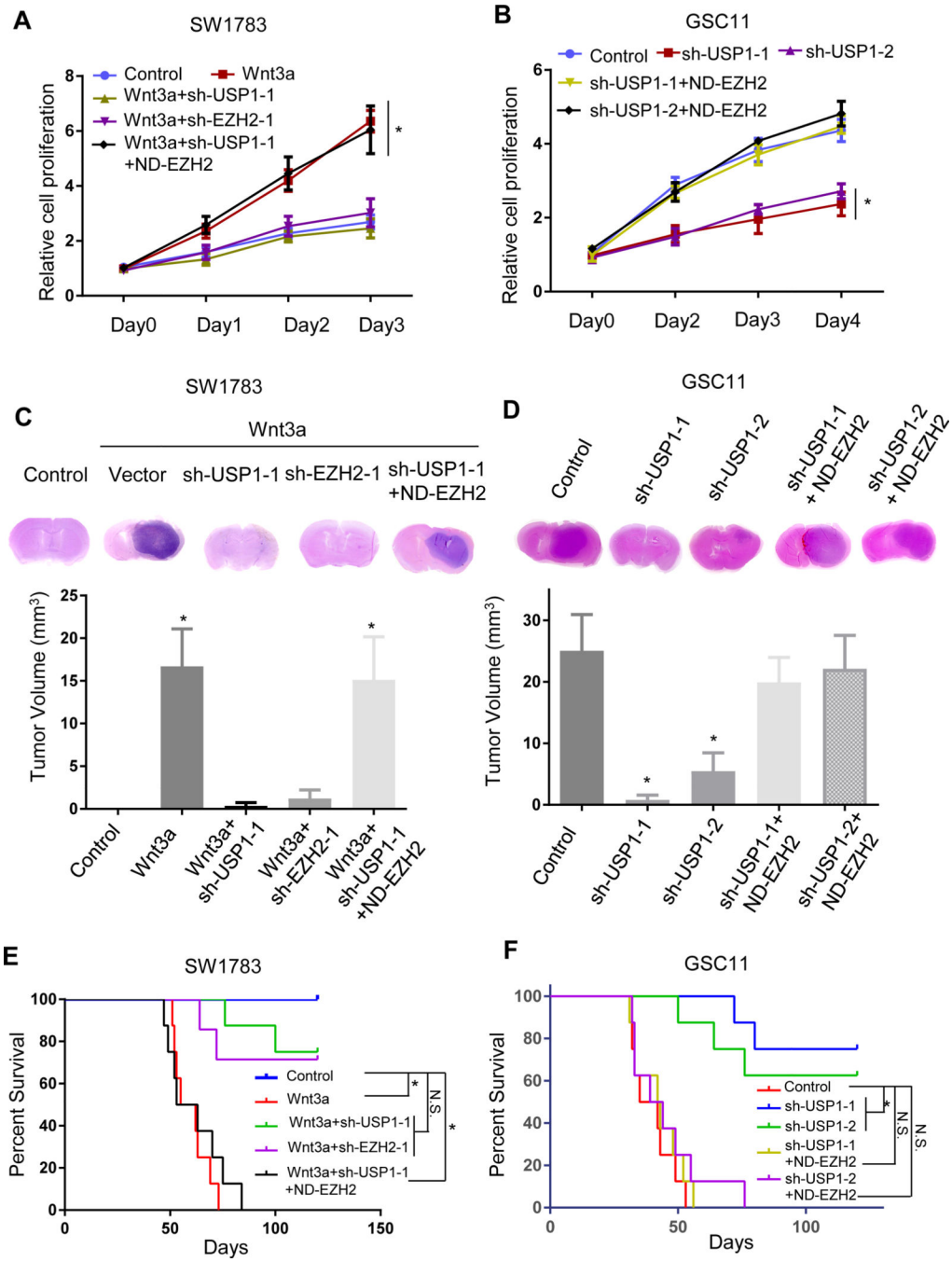


**Fig. 6. β-Catenin-USP1-EZH2 axis promotes glioma cell growth and tumorigenesis.**

**(A) and (B)** Cell proliferation of SW1783 (A) and GSC11 (B) expressing the indicated constructs was assessed by XTT assays. Data were mean ± s.e.m., n=3 independent experiments, paired Student's t-test. *P<0.05, compared with control group. **(C)**SW1783 cells ($1\times10^6$ cells/mouse) expressing the indicated constructs were intracranially injected into nude mice. Six weeks after injection, the mice were humanely killed and tumor formation was assessed. **(D)** GSC11 cells ($5\times10^5$/mouse) expressing Control, sh-USP1–1, sh-USP1–2, sh-USP1–1+ND-EZH2 and sh-USP1–2+ND-EZH2 were intracranially injected

into nude mice. Four weeks after injection, the mice were humanely killed and tumor formation was assessed. Representative tumor xenografts of hematoxylin and eosin–stained sections are shown. In (C) and (D), tumor volumes were calculated as indicated in the Method. Values are mean ± s.d., n = 6 mice for each group, one-way ANOVA test. *P<0.01, compared with control group. **(E)** and **(F)** SW1783 ( E) or GSC11 (F) cells expressing the indicated constructs were intracranially injected into nude mice respectively. The survival of mice were evaluated (n=8 mice for each group, Kaplan–Meier model with two-sided log-rank test. *P<0.01, N.S. not significant, compared with control group).

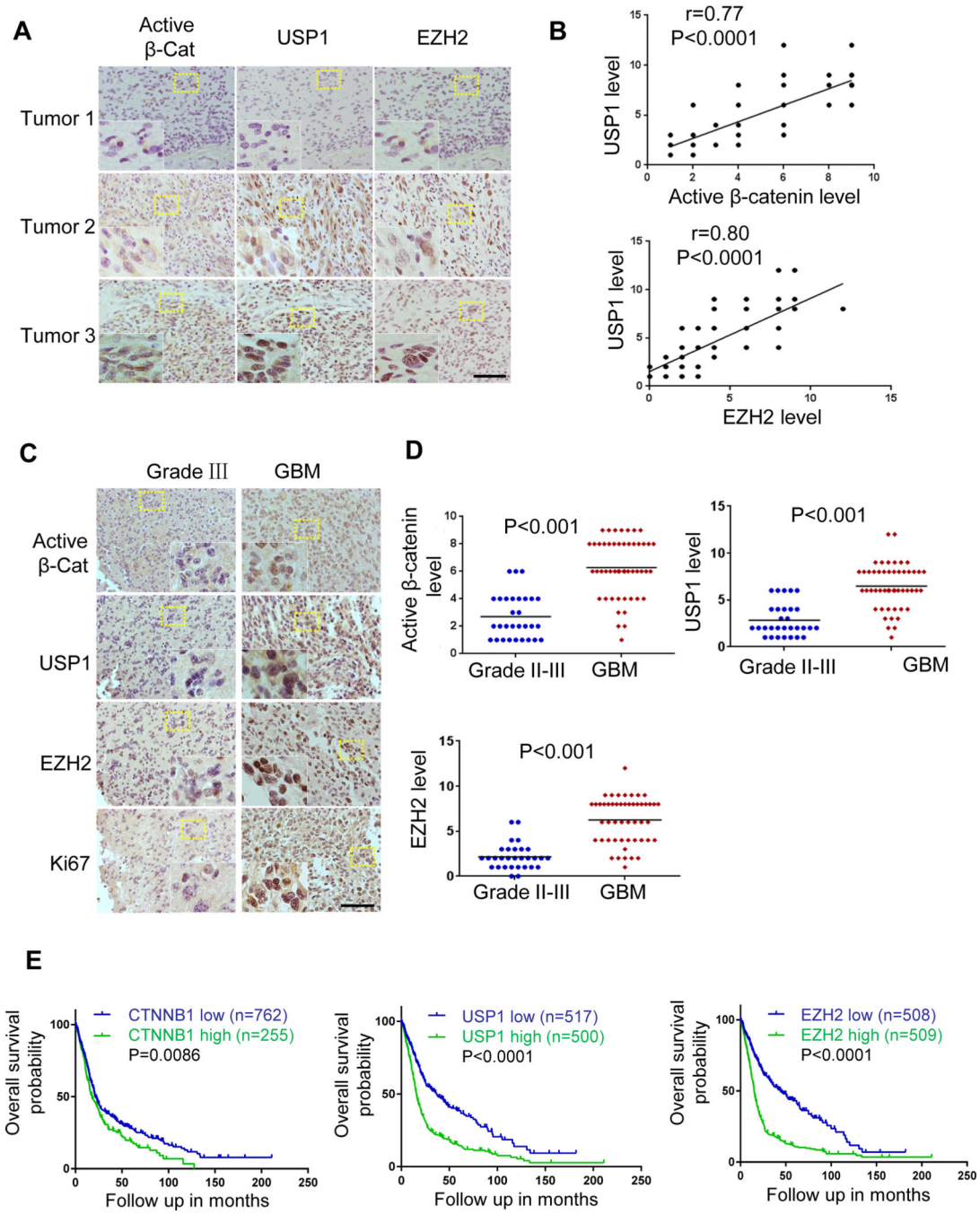


**Fig. 7. USP1 is upregulated in glioma specimens and correlates with β-catenin activation and EZH2 protein level.**

**(A)** Immunohistochemical staining of active β-catenin, USP1, EZH2 on 30 grade II-III astrocytoma and 50 GBM specimens. Representative images of three tumors were shown. Scale bar, 100 μm. **(B)** Immunohistochemical staining of active β-catenin, USP1 and EZH2 were scored on a scale of 1–12. Correlation between the expression scores of USP1 and active β-catenin/EZH2 was statistically analyzed by Pearson correlation test. Note that the scores of some samples overlap. **(C)** Immunohistochemical staining of active

β-catenin, USP1, EZH2 and Ki67 were carried out on 30 grade II-III astrocytoma and 50 GBM specimens. Representative images of staining were shown. Insets: high-magnification images corresponding to the areas marked by yellow dotted lines. Scale bars, 100 μm. **(D)** Immunohistochemical staining of active β-catenin, USP1 and EZH2 were scored on a scale of 1–12. The expression levels of active β-catenin, USP1 and EZH2 in thirty grade II-III astrocytoma were compared with those in fifty GBM specimens (unpaired Student's t test, two tailed). **(E)** Kaplan-Meier plot of glioma patients in merged TCGA datasets. Patients were subdivided into 2 groups with a cut-off value at the median USP1 or EZH2 expression, or with a cut-off value at the 75% CTNNB1 expression.